American Mineralogist, Volume 66, pages 369-375, 1981

Bartonite, a new potassium iron sulfide mineral

GERALD K. CZAMANSKE, RICHARD C. ERD

U.S. Geological Survey
345 Middlefield Road
Menlo Park, California 94025

B. F. LEONARD

U.S. Geological Survey
Federal Center
Denver, Colorado 80225

AND JOAN R. CLARK

U.S. Geological Survey
345 Middlefield Road
Menlo Park, California 94025

Abstract

The new mineral bartonite has been found in a mafic, alkalic diatreme at Coyote Peak, Humboldt County, California. Associated with it are the two previously known potassium iron sulfide minerals, djerfisherite, $K_6(Fe,Cu,Ni)_{24}S_{26}Cl$, and rasvumite, KFe_2S_3, as well as erdite, $NaFe_2S_3 \cdot 2H_2O$, and one or two other new sodium iron sulfide minerals.

Bartonite has been found in discrete segregations of sulfide in which pyrrhotite predominates. It is blackish brown, distinctly darker than pyrrhotite on fresh surfaces; in polished section it is yellow, softer and darker than pyrrhotite, and anisotropic. Bartonite is tetragonal, *I4/mmm*, $a = 10.424(1)$, $c = 20.626(1)$Å, $Z = 2$; density for $K_{5.70}Fe_{21.24}S_{26.93}$ 3.366 g cm^{-3} (calc.), 3.305(10) (meas.). The six strongest lines of the X-ray diffraction powder pattern are (in Å): 2.998(100)(224), 5.99(77)(112), 1.833(40)(408), 9.31(27)(101), 3.139(27)(312), and 2.379(25)(316). Reflectance in air at 540 nm is 20.9% for R_O, 21.8% for $R_{E'}$. Microindentation hardness (VHN) at 15-gram load is 94–120, mean 104±9.

Introduction

Bartonite, djerfisherite, and rasvumite were noted in several representative polished sections of Coyote Peak material; they defied analysis and identification before we hypothesized that these yellowish green-grey sulfide phases might contain potassium. The name honors Paul B. Barton, Jr., sulfide petrologist with the United States Geological Survey, for his outstanding contributions toward rigorous utilization of sulfide mineral chemistry in the deciphering of ore genesis. Bartonite is the first sulfide mineral for which a radiometric age (29.4±0.5 m.y.) has been directly determined (Czamanske *et al.*, 1978). The new mineral and the name bartonite were approved by the Commission on New Minerals and Mineral Names of the International Mineralogical Association in November 1977.[1] Type specimens will be deposited at the National Museum of Natural History, Smithsonian Institution.

The geology and mineralogy of the diatreme at Coyote Peak have been briefly described by Czamanske *et al.* (1977, 1980).

Occurrence and paragenesis

Bartonite is typically found associated with pyrrhotite in rare sulfide-rich clots several centimeters on a side. Bartonite may constitute only 10–15 per-

[1] Note that bartonite was approved as a new mineral on the basis of the formula $K_3Fe_{10}S_{14}$, and was ascribed that formula by Czamanske *et al.*, 1978 and 1979. More cautiously, it was called "a new K, Fe-sulfide closely related to djerfisherite" by Czamanske *et al.*, 1980.

0003–004X/81/0304–0369$02.00

cent of such masses, but areas several mm in dimension may consist of equal portions of bartonite and pyrrhotite. A small amount of pyrite may also be present. Bartonite may be intimately intergrown with the typical silicates—phlogopite, schorlomite, acmite, clinopyroxene, nepheline, natrolite, and sodalite—that comprise the host rock to the sulfide-rich clots. In many specimens, textures strongly suggest that bartonite has replaced pyrrhotite (Figs. 1 through 3). However, it is unclear to what extent bartonite may also have replaced silicate matrix or, indeed, have been replaced itself by late crystallizing silicates. In places, bartonite is finely veined by one or more gangue minerals (Figs. 1 and 2), and some aggregates of bartonite contain inclusions of phlogopite and other gangue minerals.

Figures 1 and 2 show typical bartonite–pyrrhotite relations. Bartonite embays pyrrhotite, and minute veinlets or cusps of the host pyrrhotite project between individual bartonite grains. Rarely, bartonite occurs as small skeletal crystals, as subhedral cores of magnetite octahedra, and as atolls in equant inclusions of gangue in pyrrhotite.

Observation to date has not revealed the sequential relations of bartonite to the other K and Na sulfides—djerfisherite, rasvumite, erdite ($NaFeS_2 \cdot 2H_2O$), and $NaFe_3S_5 \cdot 2H_2O$—as it has not been seen with them.

Pyrrhotite, typically the dominant sulfide in bartonite-bearing assemblages, occurs as irregular masses and occasionally as tabular crystals. This pyrrhotite contains 47.3 atomic percent Fe (wt.%; Fe = 61.2±0.3, S = 39.1±0.3), and X-ray study shows that it is a 5*C*, ordered hexagonal pyrrhotite (Carpenter and Desborough, 1964).

Pyrite commonly occurs as fine-grained aggregates replacing pyrrhotite along fractures. It also occurs sparingly as veinlets in bartonite, as enclosures in gangue minerals that vein bartonite, as fringes of minute prisms on bartonite, and as small patches between bartonite and pyrrhotite. Bartonite has partially altered to goethite on one specimen.

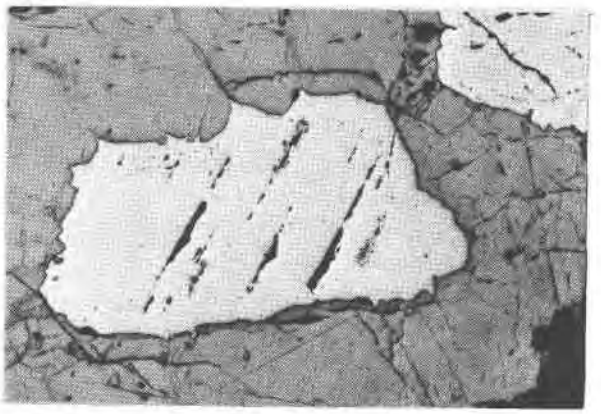

Fig. 2. Bright pyrrhotite, interpreted as a residual cuspate island being replaced by bartonite. 77-CYP-31, 1.06 × 1.50 mm.

Aggregates of acicular, high-iron sphalerite (blades to 0.5 × 0.02 mm) are present in bartonite in one sample; analyses show (wt.%) Fe = 24±1, Mn = 1.3, Cd = 1.0. Also present is a subhedral skeletal crystal of loellingite (0.09 × 0.17 mm) containing 1.6 wt.% Ni.

Small octahedra and platelets of magnetite are studded throughout some aggregates of bartonite and appear in some instances to be localized at bartonite–pyrrhotite contacts (Fig. 3). Trains of magnetite octahedra are much less frequently seen in pyrrhotite. Titaniferous magnetite is an important constituent in the host rock, but the fine-grained magnetite associ-

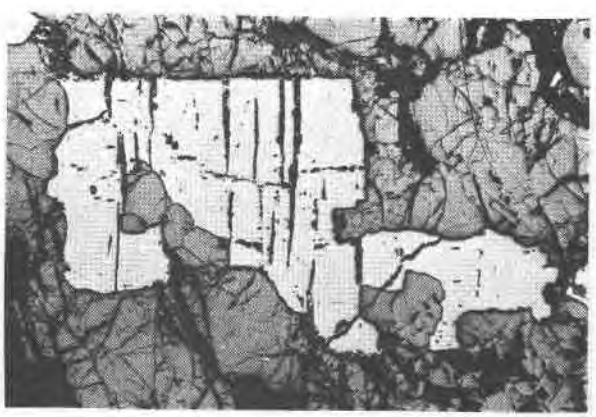

Fig. 1. An irregular remnant of bright pyrrhotite in a matrix of bartonite veined by silicates. 77-CYP-15, 1.37 × 1.94 mm.

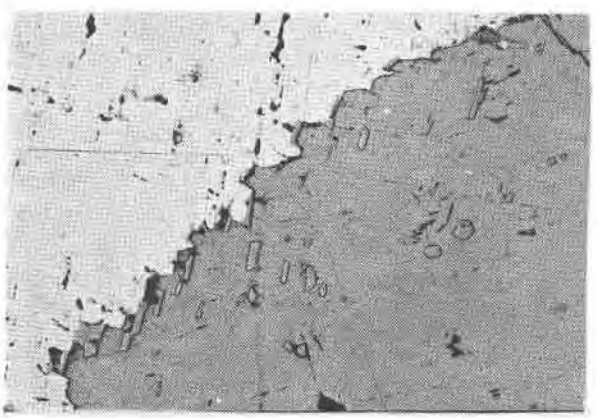

Fig. 3. Concentration of sharply bounded, fine-grained magnetite along interface between pyrrhotite (bright) and bartonite, 77-CYP-31, 0.72 × 1.00 mm.

ated with bartonite and erdite (Czamanske *et al.*, 1979) is nearly free of Ti and is interpreted to be a later reaction product, perhaps partially in accommodation of iron released by replacement of pyrrhotite (atomic Fe/S = 0.899) by bartonite (Fe/S = 0.762–0.785).

Composition

Analyses of bartonite and associated K, Fe-sulfide phases were made on the ARL EMX-SM electron microprobe at Menlo Park, California. (Analytical details are noted in the footnote to Table 1). Aside from the somewhat more massive occurrence and replacement relation to pyrrhotite, the strongest indication that we were dealing with a phase distinct from djerfisherite was in the lower metal-to-sulfur ratio characteristic of bartonite. Subsequent study has shown that this distinction may be uncertain because bartonite composition appears to vary.

The composition of chlorine-poor bartonite is represented by the five analyses (from two specimens) averaged in Table 1; included is an analysis made on the crystal fragment from which the single-crystal data were collected for the structural analysis (Evans and Clark, 1981). Refinement of site populations in the crystal structure analysis of the selected crystal fragment gives the formula $K_{5.68}Fe_{20.27}S_{26}(S)_{0.93}$, in good agreement with the microprobe analysis of that crystal, $(K,Na)_{5.70}(Fe,Ni,Co,Cu)_{21.24}S_{26.93}$ (included in Table 1). We believe that chlorine-poor bartonite is most abundant.

Existence of a chlorine-rich variety of bartonite is postulated on the basis of the data presented in the upper part of Table 2. These data represent small, optically indistinguishable areas a few tenths mm on a side, contiguous with Cl-poor bartonite. The high sulfur content, considered to be a distinction between bartonite and djerfisherite, is maintained. Notable, in

Table 1. Electron microprobe analyses of Cl-poor bartonite from Coyote Peak, Humboldt County, California (weight percent).

	Bartonite (5)*	Calculated $K_{5.68}Fe_{20.27}S_{26.93}$**
K	9.54 (9.44- 9.71)	10.01
Na	0.05 (0.02- 0.14)	-
Fe	51.2 (50.8- 51.8)	51.05
Ni	0.19 (0.10- 0.31)	-
Co	0.11 (0.07- 0.17)	-
Cu	0.62 (0.56- 0.66)	-
S	38.4 (37.6 -39.1)	38.94
Cl	0.02 (0.01- 0.02)	-
	100.13	100.00
D calc. (g/cm^3) for Z=2	3.333	3.286

*Indicates number of discrete areas analyzed (6-8 points counted) in specimens 15 and 31. Initial values are averages over indicated ranges. Analyses at 15KV and 0.02 amp sample current using as standards: K, biotite for rasvumite and natural, Khibina rasvumite for the other K-Fe-S minerals; Na, natural crocidolite; Fe and S, synthetic FeS; Ni, synthetic monosulfide solid solution (mss) containing 9.89 wt.% Ni; Co, synthetic mss containing 4.09 wt.% Co; Cu, natural chalcopyrite; Cl, natural sodalite. Data were corrected by the theoretical scheme FRAME (Yakowitz et al., 1973). Identical procedures were used to obtain the data of Table 2.

**From structural analysis by Evans and Clark (1981).

Table 2. Electron microprobe analyses of Cl-rich bartonite, djerfisherite, rasvumite, and phases apparently intermediate to bartonite and djerfisherite.

	Cl-rich bartonite					
	15*				D4A	
K	10.5(.2)**	10.6	10.5	10.3	10.4	10.5
Na	-***	-	-	0.22(.02)	0.20	0.20
Fe	50.3(.4)	48.7	48.7	48.2	49.0	46.8
Ni	0.25(.03)	0.46	0.43	0.42	0.04	0.16
Cu	0.52(.03)	0.66	0.77	0.81	0.93	3.36
S	37.3(.6)	38.1	38.2	37.9	38.0	38.0
Cl	1.35(.05)	1.38	1.30	1.23	0.78	0.82
Σ	100.22	99.90	99.90	99.08	99.35	99.84

	Intermediate Phases						
	125A				9	134	
K	10.6	10.5	10.1	9.10	9.15	9.20	9.30
Na	0.64	0.52	0.34	0.06	-	0.78	0.58
Fe	47.2	46.7	47.1	46.3	44.4	45.7	49.8
Ni	0.60	1.30	1.51	0.95	2.37	1.36	0.08
Cu	4.44	5.12	3.80	7.72	7.86	5.16	2.98
S	34.4	35.0	35.4	35.6	35.7	36.3	36.3
Cl	0.95	0.80	0.79	0.00	0.00	1.20	1.02
Σ	98.83	99.94	99.04	99.73	99.48	99.70	100.06

	Djerfisherite					Rasvumite
	125A	134		133		133
K	9.30	9.20	9.00	9.10	9.45	15.8
Na	0.07	0.76	0.76	0.04	0.10	0.02
Fe	47.9	45.4	45.4	45.0	44.2	45.6
Ni	1.64	1.31	1.41	0.87	0.76	0.01
Cu	4.92	6.91	8.37	9.21	9.69	0.00
S	34.4	34.8	33.8	34.5	33.8	38.6
Cl	0.80	1.20	1.26	1.18	1.13	0.01
Σ	99.03	99.58	100.00	99.90	99.13	100.04

*Sample numbers presented to allow insight into phase association.

**Indicates estimated uncertainty. For each analysis 6-8 points were occupied for each distinct mineral phase.

*** - indicates not sought.

addition to the increased Cl, are the higher content of K and a distinctly lower summation for Fe + Ni + Cu (see Table 3). We have been unable to develop a crystal-chemical argument that convincingly explains this apparent relation between contents of Cl, K and Fe + Ni + Cu. As shown in Table 3, compositional data for Cl-bartonite are best matched by the formula $K_6Fe_{20}S_{26}(S_{0.25}Cl_{0.75})$.

The middle row of Table 2 presents data for substances which appear to be neither bartonite nor djerfisherite. All seven analyses show more metal and less S than bartonite, and all show significantly more Ni + Cu than all but one of the analyses ascribed to bartonite. On the other hand, three of the analyses contain too much K for djerfisherite, two contain no Cl, and the remaining two have S contents that are well above those expected for djerfisherite. We offer two suggestions, which differ chiefly in scale: (1) perhaps the individual, close-packed layer stackings typical of bartonite and djerfisherite (Evans and Clark, 1981, Fig. 1) are intermingled in hybrid fashion; or (2) perhaps the phases are intergrown on a submicroscopic scale. In contrast to bartonite, which occurs in substantial masses with millimeters of continuity, djerfisherite and these possible intermediate substances occur as fine, interstitial disseminations amid silicates or as thin "skins" on late "pegmatitic" silicate crystals (*e.g.,* phlogopite). Thus, there has been no opportunity to conduct comparative single-crystal studies of these phases.

The lower part of Table 2 presents comparative data for djerfisherite and rasvumite from Coyote Peak. The djerfisherite analyses are typical of those published for other localities (Czamanske *et al.,* 1979). The fact that djerfisherite seems to accommodate substantially more Ni and Cu than bartonite is probably related to differences in bonding within the Fe_8S_{14} cube clusters of the two minerals, despite their close structural similarity (Evans and Clark, 1981). In our experience, rasvumite is the purest K, Fe-sulfide mineral (Czamanske *et al.,* 1979). It seems probable that the double edge-sharing chains of Fe–S tetrahedra, characteristic of this orthorhombic mineral (Clark and Brown, 1980), are even less accommodating to substitutions than the bartonite cube clusters.

Table 3. Average Cl-rich bartonite composition compared to theoretical formulae.

	Cl-rich bartonite*	$K_6Fe_{20}S_{26}/(S_{0.25}Cl_{0.75})$	$K_6Fe_{20}S_{26}/(S_{0.5}Cl_{0.5})$	$K_6Fe_{21}S_{26}/(S_{0.25}Cl_{0.75})$
K	10.46	10.57	10.57	10.30
Na	0.21	---	---	---
Fe	48.98	50.32	50.34	51.54
Ni	0.32	---	---	---
Cu	0.74	---	---	---
S	37.90	37.91	38.29	36.93
Cl	1.21	1.20	0.80	1.17
Σ	99.82	100.00	100.00	100.00
D calc. g/cm³ for Z=2	3.283	3.289	3.288	3.372

*Average excludes the single high-Cu bartonite (?) analysis of Table 2.

From both a paragenetic and crystal-chemical view, it is interesting to consider what factors might control crystallization of the three K,Fe-sulfide minerals, djerfisherite, bartonite, and rasvumite. The most obvious clue is in the apparent oxidation state of Fe. Assuming that all S is 2−, iron is fully reduced in djerfisherite, has a valence of 2.50 in rasvumite, and in bartonite has a formal valence of 2.27 in $K_{5.7}Fe_{21.2}S_{26.9}$ and 2.36 in $K_6Fe_{20}S_{26.1}(S_{0.25}Cl_{0.75})$. The structures and occurrence of these minerals may thus reflect the oxidizing potential in the environment in which they formed. This explanation fits reasonably well with the occurrence of these phases at Coyote Peak. The common occurrence of djerfisherite as disseminated fine grains amid silicates suggests early crystallization, whereas bartonite occurs in replacement relation to earlier pyrrhotite. In contrast, bundles of rasvumite needles (Czamanske *et al.,* 1978) typically occur in small pegmatitic clots that seem to have formed at a late stage. Rasvumite is associated with the Na,Fe-sulfide phases in which iron is also fully oxidized, and erdite replaces djerfisherite. From another perspective, it could be said that the K,Fe-sulfide minerals suggest an oxidizing trend during consolidation of the Coyote Peak diatreme.

Chemical properties

Bartonite is readily soluble with effervescence in hot concentrated HNO_3 and soluble with difficulty and effervescence in hot concentrated HCl. When heated in a closed tube, it gives off sulfur and turns black. Its initial decomposition product is pyrrhotite; with continued heating in a platinum crucible, it is oxidized to hematite.

Crystallography

Unit-cell dimensions were determined from precession photographs (Zr-filtered Mo radiation) of the

*hk*0, 0*kl*, *hhl*, and *hkl* nets. Extinctions in these photographs lead to the diffraction aspect *I*/4***; crystal structure study (Evans and Clark, 1981) shows the space group to be *I*4/*mmm*. The cell dimensions given in Table 4 were refined by least-squares analysis of the X-ray powder data using the computer program of Appleman and Evans (1973). Calculated intensities obtained from the crystal structure study of Evans and Clark are given in Table 5 and have been used to index the data.

The X-ray powder diffraction data (Table 5) are similar to those of djerfisherite (Fuchs, 1966; Genkin *et al.*, 1969) but may easily be distinguished by the presence of additional lines, the strongest of which are at 9.31, 3.139, 2.389, 2.374, and 1.833Å.

Bartonite typically occurs as anhedral masses. A few single crystals are present in patches of fine-grained silicate matrix and as parallel intergrowths with coarse acmite. The crystals, less than 5 μm wide and 5 to 10 times as long, are prisms, some of them terminated at one end by a pyramid or by a pyramid and the basal pinacoid. The opposite ends of these prisms are gently curved or ragged. The form {112} was identified on an exceptional crystal fragment.

Physical properties

Bartonite occurs as blackish-brown anhedral masses with a submetallic luster and a black streak. It has a conchoidal fracture. In polished sections a distinct cleavage {112} was noted on some sections lying parallel to the prism axes of rare microcrystals.

Table 4. Unit-cell data for bartonite

Space Group	I4/mmm
a (Å)	10.424(1)
c	20.626(1)
V (Å^3)	2241.2(3)
c/a	1.979
Cell content, from structural analysis**	2[$K_{5.68}Fe_{20.27}S_{26.93}$]
Density (calc.)	3.286 gcm^{-3}
Specific gravity (meas.)	3.305(10)*

*Determined at 25°C by suspension in methylene iodide-acetone.
**Evans and Clark (1981).

Table 5. X-ray powder diffraction data for bartonite, Coyote Peak, Humboldt County, California

hkl	Calculated* d_{hkl} (Å)	I	Observed** I	Observed** d_{hkl} (Å)
002	10.313	16	15	10.31
101	9.303	68	27	9.31
110	7.371	12	8	7.38
112	5.997	58	77	5.99
103	5.739	7	8	5.74
105	3.836	6	---	---
006	3.438	4	---	---
301	3.426	15	12	3.428
310	3.296	9	15	3.296
312	3.140	32	27	3.139
116	3.115	14	15	3.116
303	3.101	6	10	3.102
224	2.998	100	100	2.998
206	2.870	3	8	2.863
321	2.863	4		
107	2.835	9	6	2.837
411	2.509	6	6	2.510
332	2.390	18	17	2.389
316	2.379	40	25	2.379
406	2.077	2	8	2.075
431,501	2.074	5,2		
512	2.005	8	6	2.000
336	1.999	3		
11·10	1.986	4	6	1.987
435,505	1.861	4,1	4	1.860
440	1.843	41	25	1.841
408	1.833	79	40	1.833
532	1.761	4	---	---
516	1.757	4	---	---
437	1.702	3	8	1.698
419	1.698	3		
624	1.570	14	12	1.570
22·12	1.558	6	4	1.557
712	1.459	4	2	1.459
800	1.303	9	2	1.302
00·16	1.289	4	2	1.288
736	1.272	5	2	1.272

*Calculated spacings listed for d_{hkl} ≥5.500Å. Indices from least-squares analysis of X-ray powder data using the program of Appleman and Evans (1973). Calculated intensities from computer program POWDER (I. C. Jahanbagloo, unpubl. 1964, revised 1969, Univ. Rochester, New York) using preliminary atomic coordinates (Evans and Clark, 1980), and intensities normalized with (224) = 100.

**Specimen No. 77-CYP-15. X-ray diffractometer conditions are: chart no. X-4309; Cu/Ni radiation; λCuK_{α_1} = 1.540598Å; silicon used as internal standard; scanned at 1/4° minute from 4-80° 2θ.

The cleavage trace is at 45° to *c* on {010} sections. This cleavage has not been observed on larger grains. Variously oriented fractures dissect many of the prisms. The trace of one set of persistent fractures is nearly perpendicular to the prism edge.

The microindentation hardness of bartonite at a load of 15 g is 94.0–120, mean 104±9. Measurements of 9 grains were made with the Vickers diamond pyramid of a Letiz Durimet hardness tester. All indentations are nearly equant and of a very good quality. The Mohs hardness is 3½. Bartonite takes a

good polish, but at a magnification of 150× some extremely fine scratches are visible. The polishing hardness is much less than that of pyrrhotite.

Bartonite is weakly magnetic (somewhat less magnetic than ilmenite) and may easily be distinguished by this property from the associated pyrrhotite, which is much more strongly magnetic. Its specific gravity (3.305; Table 4) aids in distinguishing it from djerfisherite, which has a specific gravity of about 3.9.

Optical properties

In polished section, bartonite aggregates isolated by the field diaphragm are yellow, neither bright nor dark according to BFL, and appear brownish yellow to GKC. Reflection pleochroism is barely perceptible. Anisotropism is distinct, almost without tint. Internal reflection is absent. Extinction is parallel to the prism edge. Against pyrrhotite, bartonite is yellowish green gray, or yellowish green brown, at first glance resembling greenish members of the tennantite-tetrahedrite series but somewhat darker than these and much darker than pyrrhotite. Against pyrite, bartonite is slightly greenish yellow and much darker. In oil, isolated aggregates of bartonite seem little changed, but bartonite next to pyrrhotite appears greenish gray or greenish brown and much darker. In a maritime climate, bartonite shows no tarnish months after polishing.

The reflectance of two groups of bartonite grains is given in Table 6. Substantial differences in reflectance behavior are evident from grain to grain within the two groups. How much of the difference is due to slight variation in composition and how much to the vagaries of polishing and measuring, we do not know. For some bartonite grains, the reflectance is higher in the middle of the spectrum than at 470 and 650 nm; for other grains, reflectance increases with increasing wavelength, or increases from 470 to 589 nm and then remains constant. Because a selection of good crystals of known orientation is not available, we do not know if the few highly bireflecting grains are aberrant or if they more nearly represent the true bireflectance of the mineral.

Two grains of bartonite were used for measurements of R_O and R_E throughout the visible spectrum (Table 7). These grains were chosen because they were best polished, not because they showed the highest bireflectance. The bartonite grains of Table 7 are optically positive throughout most of the spectrum, but they are optically negative at wavelengths below 455 nm. At 455 nm, they are isotropic. Reflectance measurements made at 400–500 nm on additional bireflecting grains differ somewhat in absolute values of R_O and R_E, but confirm the presence of crossed dispersion in the blue. The phenomenon of crossed dispersion of reflectance (equivalent in uni-

Table 6. Reflectance of groups of bartonite grains, measured at standard wavelengths.

	R^{air}, %			
	470	546	589	650 nm
A. Cl-poor (3 grains)				
R, range	20.2-21.9	25.2-29.0	24.8-28.0	22.7-25.6
$\bar{R}_1 = R_O$**	20.8±0.8	27.3±1.9	25.9±1.7	24.2±1.3
$\bar{R}$**	20.9±0.7	27.5±1.6	26.0±1.4	24.4±1.1
R_2-R_1, max.	0.3	0.6	0.5	0.7
B. Unanalyzed (4 grains)				
R, range	18.2-22.0	21.3-28.5	22.5-28.2	24.0-25.4
$\bar{R}_1 = R_O$	19.4±1.5	23.2±3.0	24.1±2.2	24.6±0.7
$\bar{R}$	19.8±1.4	23.7±2.8	24.6±2.1	24.9±0.8
R_2-R_1, max.	1.3	1.4	1.8	1.5

*Reflectance measured by B. F. Leonard with a Zeiss MPM microphotometer fitted with a Smith vertical illuminator and a Veril type-S running interference filter whose half-width at half-height is ~10 nm. Objective 16x Pol, N.A. 0.35. Zeiss-calibrated SiC standard no. 052. Mounts press-leveled on plasticine. Final polish with 0.05-μm alumina in water on Buehler microcloth. Reproducibility of individual measurements is ±1% relatively.

**Mean and standard deviation $\bar{s}$.

Table 7. Reflectance of two bartonite grains, measured at 20-nm intervals. (Measured on two separate grains, one isotropic, the other anisotropic. R_O of both grains identical at standard wavelengths of 470, 546, 589, and 650 nm. For conditions of measurement, see Table 6.)

	R^{air}, %	
Wavelength, nm	$R_1 = R_O$	$R_2 = R_E'$
400	21.7	18.3
420	16.7	14.4
440	17.7	17.2
460	18.4	18.6
480	19.4	19.5
500	19.7	20.6
520	20.3	21.4
540	20.9	21.8
560	21.9	22.7
580	22.7	23.2
600	23.4	23.7
620	23.9	24.3
640	24.7	25.1
660	25.0	25.5
680	25.2	26.1
700	26.4	26.5

Table 8. Quantitative color designation of bartonite referred to I.C.I. illuminant C. (Method of 30 selected ordinates.)

	x	y	Y,%	λ_d,nm	p_e,%
R_O	0.333	0.335	21.7	581	11.2
$R_{E'}$	0.335	0.342	22.4	577	13.6

axial substances to change of optic sign) is common among ore minerals, though it has seldom been reported for minerals of low bireflectance.

Provisional values of n and k for the anisotropic grain of Table 7 were obtained by calculation from measurements of R^{air} and R^{oil} against the calibrated SiC standard. At 589 nm, $R_O = 23.3_5$, $R_{E'} = 23.7\%$ in air; $R_O = 11.3$, $R_{E'} = 11.6\%$ in oil at 24.6°C. Thus, $no = 2.22$, $ko = 1.10$, $nE' = 2.22_5$, $kE' = 1.12$. The oil used was Cargille D/N 58.884; $n^{23°}$ (589) = 1.5151±0.0002, independently determined by Ray E. Wilcox, U.S. Geological Survey. Because small errors in the measurement of reflectance substantially affect the calculated values of n and k, we emphasize that the values given for the single bartonite grain are provisional. Note that the values cited for R^{air} in this paragraph were obtained by remeasurement, not by interpolation from Table 7. Therefore, R^{air} is validly paired with R^{oil} in deriving n and k. To produce a valid set of measurements some time after obtaining the data of Table 7, it was necessary to repolish the specimen, retrieve the grain needed, remeasure R^{air}, and immediately measure R^{oil}. Such a precaution can control some of the variables that enter in to the measurement of reflectance, but it cannot ensure that the derivative values n and k are correct.

Quantitative color data calculated for the bartonite grains of Table 7 are given in Table 8. These data, derived from microphotometry and selectively integrated over the visible spectrum, define a yellow of rather low brightness and low excitation purity. The color definition agrees fully with BFL's visual impression of the color of isolatable grains of bartonite: yellow, neither bright nor dark.

The observation that bartonite looks yellowish green against pyrrhotite can be explained by referring to the reflectance curves of the two minerals. Curves for hexagonal pyrrhotite can be plotted from reflectances measured by K. v. Gehlen and H. Piller (Henry, 1977, card no. 1.7240.2; or by Vyal'sov, 1973). When the curves of the two minerals are compared, it is evident that the reflectance curves of bartonite, relative to those of hexagonal pyrrhotite, flatten in the 500–540 nm region. Therefore, the eye focused on bartonite adjacent to pyrrhotite sees green or yellowish green, not yellow. The effect is enhanced because bartonite has the greater excitation purity; that is, regardless of the hue sensed by the observer, the saturation is intrinsically greater for bartonite.

Acknowledgments

The counsel of Howard T. Evans, Jr. has been especially valuable to us throughout this study. We also thank him, Priestley Toulmin III, A. J. Criddle, and J. Chisholm for perceptive reviews of the manuscript.

References

Appleman, D. E. and Evans, H. T., Jr. (1973) Job 9214: Indexing least-squares refinement of powder diffraction data. U.S. National Technical Information Service, Document PB–216 188.

Carpenter, R. H. and Desborough, G. A. (1964) Range in solid solution and structure of naturally occurring troilite and pyrrhotite. American Mineralogist, 49, 1350–1365.

Clark, J. R. and Brown, G. E. (1980) Crystal structure of rasvumite, KFe_2S_3. American Mineralogist, 65, 477–482.

Czamanske, G. K., Erd, R. C., Sokolova, M. N., Dobrovol'skaya M. G., and Dmitrieva, M. T. (1979) New data for rasvumite and djerfisherite. American Mineralogist, 64, 776–778.

Czamanske, G. K., Lanphere, M. A., Erd, R. C., and Blake, M. C., Jr. (1978) Age measurements of potassium-bearing sulfide minerals by the Ar^{40}/Ar^{39} technique. Earth and Planetary Science Letters, 40, 107–110.

Czamanske, G. K., Leonard, B. F., and Clark, J. R. (1980) Erdite, a new hydrated sodium iron sulfide mineral. American Mineralogist, 65, 509–515.

Czamanske, G. K., Meyer, C. E., Erd, R. C., and Norman, M. B., II (1977) The Coyote Peak diatreme, Humboldt County, California. (abstr.). EOS, 58, 1247.

Evans, H. T., Jr. and Clark, J. R. (1981) The crystal structure of bartonite, a potassium iron sulfide, and its relationship to the structures of pentlandites and djerfisherites. American Mineralogist, 66, 376–384.

Fuchs, L. H. (1966) Djerfisherite, alkali copper-iron sulfide: a new mineral from enstatite chondrites. Science, 153, 166–167.

Genkin, A. D., Troneva, N. V., and Zhuravlev, N. N. (1969) The first occurrence in ores of the sulfide of potassium, iron, and copper—djerfisherite. Geologii Rudnykh Mestorozhdenii, 11, No. 5, 57–64.

Henry, N. F. M. (Ed.) (1977) IMA/COM Quantitative data file. International Mineralogical Association, Committee on Ore Microscopy, London.

Vyal'sov, L. N. (1973) Spektry otrazheniya rudnykh mineralov [Reflectance spectra of ore minerals]. Moskva, Akademiia Nauk SSSR, Institut Geologii Rudnykh Mestorozhdenii, Petrografii, Mineralogii i Geokhimii.

Yakowitz, H., Myklebust, R. L., and Heinrich, K. F. J. (1973) FRAME: An on-line correction procedure for quantitative electron probe analysis. U.S. National Bureau of Standards Technical Note 796.

Manuscript received, July 7, 1980;
accepted for publication, October 22, 1980.